RSC Advances

PAPER

View Article Online
View Journal | View Issue

Cite this: *RSC Adv.*, 2026, **16**, 10088

A novel cyan-emitting fluorescent α-amino acid: synthesis, photophysical characterization and live-cell imaging properties

Aakash Gupta, [a] Bing Yan,[a] Yu Hsiang Cheng[a] and Maolin Guo *[ab]

Small-molecule-based fluorescent probes, particularly fluorescent analogs of α-amino acids (FAAs), have become valuable tools for labeling proteins of interest and visualizing biological processes in living cells. In this study, we report the design, synthesis, and characterization of a novel cyan-emitting fluorescent α-amino acid, 4-dibenzothiophen-4-yl-L-phenylalanine (DBT-FAA). DBT-FAA was synthesized in good yield *via* a facile 3-step procedure involving modified Suzuki–Miyaura cross-coupling and characterized by spectroscopic methods. The compound exhibits strong fluorescence in a broad range of aqueous and polar solvents, with a major emission peak at ~424–445 nm and secondary shoulders at longer wavelengths (~448–583 nm), along with a high quantum yield (Φ = 0.74 in DMSO at λ_{ex} = 380 nm and λ_{em} = 400–800 nm). DBT-FAA also demonstrates excellent photostability, showing strong resistance to photobleaching under aqueous conditions, which is essential for prolonged live-cell imaging. Confocal fluorescence microscopy confirmed that DBT-FAA is efficiently taken up by human HeLa cells, likely through an endocytic pathway, without observable cytotoxicity under the conditions studied. Once inside the cells, DBT-FAA initially accumulates in lysosomes and subsequently translocates to mitochondria with extended incubation time, suggesting dynamic intracellular redistribution. The robust optical properties, photostability, and cellular compatibility of DBT-FAA highlight its potential as a versatile fluorescent amino acid probe for real-time visualization of intracellular processes, offering promising applications in studying protein dynamics, molecular interactions, and cellular metabolism relevant to biochemistry, drug discovery, and protein engineering.

Received 20th December 2025
Accepted 10th February 2026

DOI: 10.1039/d5ra09861k

rsc.li/rsc-advances

1. Introduction

Fluorescence microscopy and the discovery of green fluorescent protein (GFP)[1] have played an indispensable role in advancing biomedical sciences over the past few decades.[2–7] The use of GFP as a fluorescent labeling probe, when fused to either the C-terminus or N-terminus of a protein of interest has enabled researchers to visualize target proteins at the subcellular level and to study their dynamics and function in living cells and whole organisms. In addition to GFP, several other strategies for tagging or labelling proteins have been developed. These include fusion protein expression and covalent attachment through self-labeling enzyme tags such as SNAP-tag (O^6-alkylguanine-DNA alkyltransferase, a 20 kDa mutant of a DNA repair enzyme that specifically reacts with benzylguanine moieties),[8–10] CLIP-tag (a variant that reacts with O^6-benzylcytosine substrates),[11] and HALO-tag (derived from the bacterial enzyme haloalkane dehydrogenase),[12,13] and an *Ec*DHFR-based system using folate analogues such as trimethoprim (TMP)-tags.[14–17] However, the relatively large size of GFP and these tagging enzymes often limit their applications.[12,18] The bulky nature of these fusion tags can disrupt the intrinsic shape, native structure, folding dynamics, and protein–protein interactions that are essential for maintaining protein functionality.[19] As a result, there is a growing need in the research community for fluorescent imaging approaches that minimize such perturbations. This challenge can potentially be addressed through the development of small molecule-based fluorescent probes, which offer compact, versatile and less invasive alternatives for studying proteins *in situ*.

Small molecule-based fluorescent probes, particularly fluorescent analogs of α-amino acids are excellent candidates for labeling proteins of interest.[19–22] In these systems, a fluorescent moiety is incorporated into natural or unnatural amino acids to enhance their photophysical properties. In the search for suitable candidates, significant efforts have been made to synthesize and incorporate α-fluorescent amino acids such as L-(7-hydroxycoumarin-4-yl) ethylglycine, dansyl and prodan amino acid analogs,[23,24] tryptophan analogs or mimics,[25,26] phenylalanine-based terphenyl unnatural amino acids,[27] β-(1-azulenyl)-L-

[a]*Department of Chemistry and Biochemistry, UMass Cranberry Health Research Center, University of Massachusetts Dartmouth, 285 Old Westport Road, Dartmouth, MA 02747, USA. E-mail: mguo@umassd.edu*

[b]*Department of Chemistry, University of Massachusetts Amherst, 710 North Pleasant Street, Amherst, MA 01003, USA*

alanine,[28] and derivatives incorporating fluorescent groups on the side chains of diaminopropionic acid (Dap) and lysine, including pyrene-, coumarin-, nitrobenzoxadiazole-, and fluorescein-based variants.[29] The incorporation of fluorescent amino acids (FAAs) offers several advantages, including their small size and minimal perturbation to the native protein structure and function.[23,24,30] Nevertheless, most of the current FAAs absorb and emit at shorter wavelengths, which limits their utility for *in vitro* and *in vivo* imaging, as being recently reviewed.[19–22,31] Short-wavelength excitation could potentially damage cells and alter protein conformation and functionality, especially during prolonged live-cell imaging experiments. Therefore, FAAs that absorb at longer wavelengths and exhibit high quantum yields are particularly desirable for site-specific incorporation into proteins, as they enable less invasive and more efficient fluorescence imaging.

Over the past decade, our laboratory has been developing fluorescent tools to monitor life-processes related to the chemical and molecular biology of living cells.[32–38] Building upon these research advances, we and others have sought to design and implement real-time protein tracking and imaging systems—conceptually akin to a "biological GPS"—using unnatural fluorescent amino acids.[22,31,38–41] In our envisioned biological GPS system, the fluorescent amino acid acts as a critical signaling unit, transmitting photonic information within live-cells to the microscope in a manner analogous to satellite-based navigation. Expanding the synthetic accessibility of novel fluorescent amino acids is therefore key to broadening the fluorescent amino acid toolbox and enhancing bioimaging capabilities. In this regard, following our previous synthesizing of the blue-emitting fluorescent amino acid Phen-AA,[39] we have successfully synthesized a cyan-emitting fluorescent amino acid, 4-dibenzothiophen-4-yl-L-phenylalanine (DBT-FAA). Herein we report on its synthesis, characterization, photophysical properties and cellular imaging applications.

2. Experimental

2.1 Chemicals

The chemicals *N*-(*tert*-butoxycarbonyl)-4-iodo-L-phenylalanine (Ambeed), 4-dibenzothiophenyl boronic acid (Oakwood Chemicals), *N*,*N*-dimethylformamide (Sigma-Aldrich), bis(triphenylphosphine) palladium(II) dichloride (Sigma-Aldrich), rhodamine B (Sigma-Aldrich), and methyl iodide (Alfa-Aesar) were purchased from the indicated sources and used without further purification. The other reagents and solvents used in syntheses were ACS grade and were purchased commercially.

2.2 Instrumentation and characterization

The ^{1}H NMR and ^{13}C NMR data were acquired on a Bruker AVANCE III HD 400 MHz high-performance digital NMR spectrometer. Chemical shifts were reported in delta (δ) unit parts per million (ppm) downfield tetramethylsilane (TMS) and analyzed on MestReNova software. The NMR data signals were acquired in DMSO-d_6 solvent with 0.03% of TMS as internal reference, where the splitting patterns represents, s = singlet, d = doublet, m = multiplet and coupling constants (J) are reported in Hertz (Hz). The molecular mass data were acquired on Waters ACQUITY UPLC-QTOF (Ultra-Pure Liquid chromatograph-Quadrupole Time of Flight) mass spectrometer using mobile phase of acetonitrile : water in an isocratic solvent of 1 : 1 over 10 minutes. UV-vis spectra were acquired on a PerkinElmer Lambda 25 spectrometer over a range of 200–800 nm wavelength. Fluorescence spectra were measured on a PerkinElmer LS55 luminescence spectrometer at 293 K. The excitation wavelength and filters settings used in all measurements are indicated in the figures. The optical rotation measurements were measured using a Rudolph Research Analytical Autopol III Automatic Polarimeter at 589 nm wavelength, at temperature 28.5 °C and at optical path length 100 mm.

2.3 Synthesis procedure

The fluorescence α-amino acid (4-dibenzothiophen-4-yl-L-phenylalanine) (DBT-FAA) was synthesized following a modified procedure involving Suzuki–Miyaura cross-coupling reactions (Scheme 1),[27,42,43] where 4-iodo-L-phenylalanine was firstly methyl protected, and then 4-dibenzothiophene boronic acid containing sulfur heteroatom was coupled with *N*-(*tert*-butoxycarbonyl)-4-iodo-L-phenylalanine methyl ester by Suzuki–Miyaura cross coupling reaction. The product (DBT-FAA, compound **5**) was formed following the deprotection of methyl ester and Boc-with base and acid, respectively. Detailed synthesis and characterization are provided in SI. Compound **5** ($C_{21}H_{17}NO_2S$): ^{1}H NMR (400 MHz, DMSO-d_6) (Fig. S1): δ 8.44–8.35 (m, 2H), 8.04–7.98 (m, 1H), 7.69 (d, J = 7.9 Hz, 2H), 7.63 (t, J = 7.6 Hz, 1H), 7.55–7.543 (m, 3H), 7.48 (d, J = 7.9 Hz, 2H), 3.50 (m, 1H), 3.26 (dd, J = 14.3, 3.7 Hz, 1H), 2.97 (dd, J = 14.2, 7.9 Hz, 1H). ^{13}C NMR (101 MHz, DMSO) (Fig. S2): δ 169.66, 138.93, 138.45, 137.67, 136.61, 136.35, 135.71, 130.52, 128.25, 127.71, 127.37, 126.14, 125.31, 123.30, 122.71, 121.46, 55.89, 39.99, 37.24. HRMS (ESI): m/z calculated for $[C_{21}H_{17}NO_2S + H]^+$: 348.0980, found: m/z: 348.0461 (and a dimer at m/z 695.1710) (Fig. S3).

2.4 Cell imaging methodology

HeLa cells (ATCC, CCL-2) were regularly cultured and maintained with the complete growth medium composing of DMEM with supplement of 10% FBS in a humid 37 °C incubator under 5% CO_2 level. The cell confluency was kept between 30% and 70% in a 25 cm^2 culture flask. To prepare for confocal experiments, HeLa cells were cultured in the flask until the confluency reached about ~70%. After the flask was rinsed with PBS twice, 2 ml 0.25% trypsin–EDTA solution was added followed by incubation in the incubator. Upon cell dissociation from the flask's wall, 2 ml complete growth medium was added to neutralize the enzyme and stop the digestion. The mixture was then transferred into a 15 ml tube and centrifuged for 3 min at 1000g. The medium was discarded to remove the residual enzyme and other waste products. 5 ml of fresh complete medium was added to the tube to resuspend the cell pellet. The same amount of cell containing medium from the tube was transferred into each of the 35-mm glass bottom dishes (Mattek, P35G-1.5-14-C), respectively, and 2 ml of the fresh complete

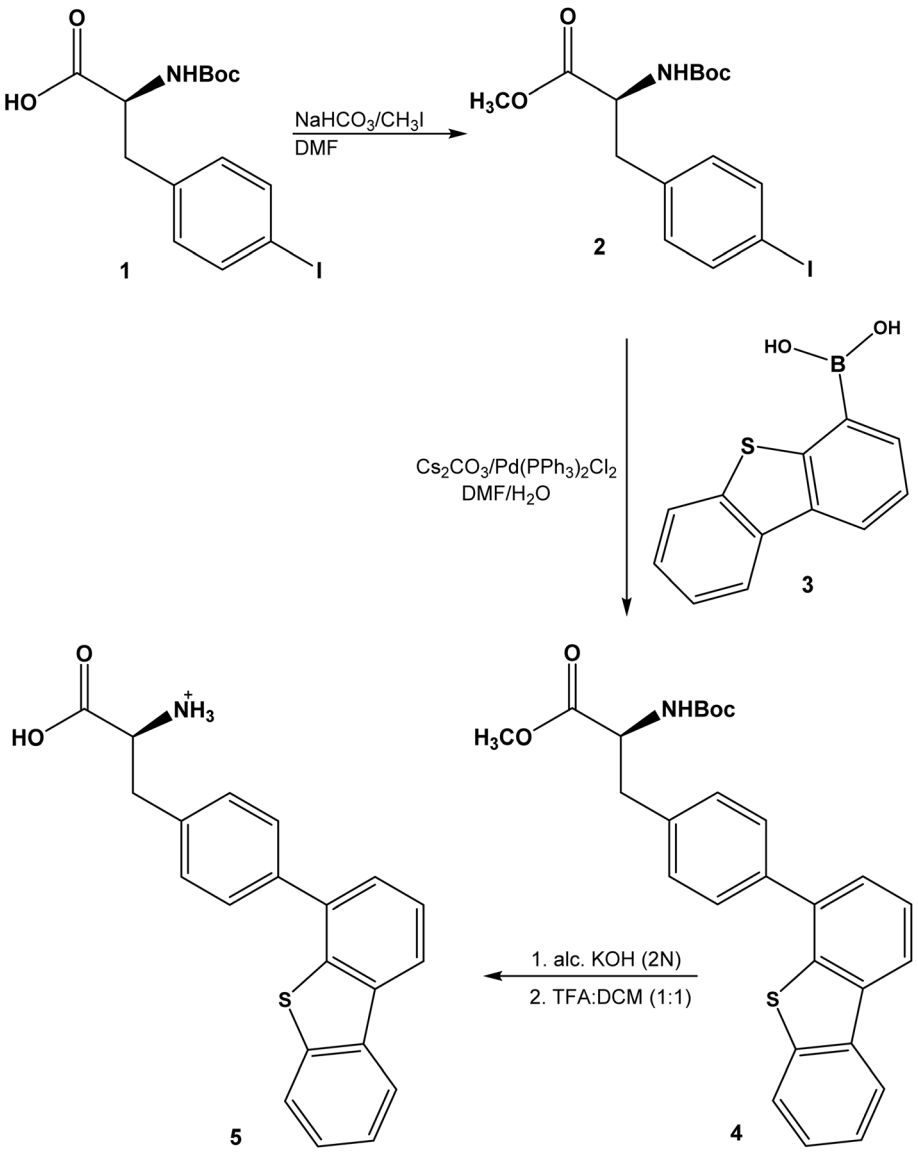

Scheme 1 Synthesis scheme of 4-dibenzothiophen-4-yl-L-phenylalanine (5, DBT-FAA).

culture medium was added, and the dishes were incubated in regular incubation condition for about 24 hours to restore normal cell condition. DBT-FAA solution (in DMSO) was added to the dishes to achieve final concentrations of 10 μM, 20 μM and 50 μM, respectively. Cells were incubated for 1 hour and washed with fresh medium before confocal experiment. For co-localization, after incubation of DBT-FAA at various time length, experiment dish was also added with MitoTracker Green (Thermo Fisher, M7514) at final concentration of 1 μM and LysoTracker RedDND-99 (Thermo Fisher, M7528) at final concentration of 1 μM and incubated for 30 min. Dish was washed with fresh medium before confocal imaging using a Zeiss LSM 710 confocal microscope.

2.5 Cell viability assay

The cytotoxicity of DBT-FAA toward human skin primary fibroblast cells (WS1, ATCC CRL-1502) was evaluated by an MTT (3-[4,5-dimethylthiazol-2-yl]-2,5 diphenyl tetrazolium bromide) assay using a MTT Cell Viability Assay Kit (Biotium, Fremont, CA, USA; cat. no. 30006). WS1 cells were cultured in Eagle's minimum essential medium supplemented with 10% fetal bovine serum (FBS) under standard conditions (37 °C, 5% CO_2). Cells were subcultured using 0.25% trypsin–EDTA and neutralized with complete growth medium. They were seeded into 25 cm^2 flasks without centrifugation, and the culture medium was replaced every 2–3 days until approximately 70% confluency was reached. Cells were then seeded into 96-well plates and incubated at 37 °C for 24 h.

The cells were treated with DBT-FAA at concentrations of 0, 10, 20, and 50 μM in 100 μL of culture medium containing 0.5% DMSO. After treatment, 10 μL of MTT solution was added to each well, mixed gently, and incubated at 37 °C for an additional 4 h. The medium was subsequently supplemented with 200 μL of DMSO, and the plate was shaken to ensure complete

dissolution of the formazan crystals. Absorbance was measured at 570 nm with background correction at 630 nm. For background subtraction, cell-free wells containing the same DBT-FAA concentrations were processed in parallel, and their signals were subtracted from the corresponding cell-containing wells. Cell viability was normalized to the 0 μM control (100%). Data are reported as mean ± SD ($n = 3$).

3. Results and discussion

3.1 Synthesis and characterization

The fluorescence amino acid 4-dibenzothiophen-4-yl-L-phenylalanine (DBT-FAA) was synthesized *via* a 3-step procedure (Scheme 1) following a modified procedure of Suzuki–Miyaura cross-coupling protocol (see SI for details). The synthetic methodology was further optimized by employing DMF as the solvent for the second step, which enhanced the solubility of the base Cs_2CO_3 and prevented the formation of side product, as confirmed by TLC monitoring. This modification resulted in an overall increase in the yield of the final product. The crude product was purified over a silica column rather than HPLC, further simplifying the synthetic process. The structure of DBT-FAA was confirmed by ^{1}H NMR (Fig. S1), ^{13}C NMR (Fig. S2), and high-resolution mass spectrometry (HRMS, Fig. S3) (see SI).

In the cyan-emitting novel fluorescent α-amino acid DBT-FAA, a thiophene ring is introduced to the side chain of a phenanthracenyl amino acid derivative.[39,44] The incorporation of a heteroatom, such as sulfur, can impart unique photophysical and physiochemical properties to the molecule. Sulfur possesses unshared electrons that can be conjugated with carbon–carbon double bonds, as well as vacant d-orbitals in its outer shell, allowing it to function both as an electron donor and acceptor. This enables its interaction with nearby charges, induces dipoles within the system, and enhances dispersion forces, polarizability, resonance energy transfer, exciplex formation, and charge transfer complexation.[45] Compared with benzene, thiophene exhibits greater hyperpolarizability and a lower aromatic delocalization energy (benzene: 36 kcal mol^{-1}; thiophene: 29 kcal mol^{-1}).[46] These electronic differences may rise to novel intermolecular interactions, including receptor–ligand binding, enzyme–substrate recognition, antigen–antibody interactions, and improved stability in mutant proteins.[45]

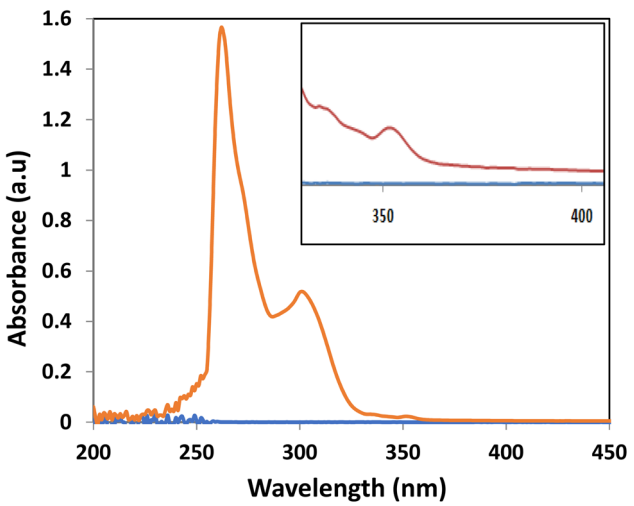

Fig. 1 UV-vis spectrum of 4-dibenzothiophen-4-yl-L-phenylalanine in DMSO (40 μM). Inset is the zoom-in of 350–400 nm region showing a long tail extended to beyond ~400 nm.

3.2 UV-vis spectroscopic analysis

The UV-vis spectrum of 4-dibenzothiophen-4-yl-L-phenylalanine (DBT-FAA) was recorded in DMSO. Analysis of its photophysical properties revealed distinct absorption features in the UV-vis spectrum (Fig. 1). The compound exhibited absorption peaks at approximately 261 nm ($\epsilon = 4.57 \times 10^4$ M^{-1} cm^{-1}) corresponding to the conjugated phenylalanine moiety, as well as additional bands at ~301 nm ($\epsilon = 1.41 \times 10^4$ M^{-1} cm^{-1}), ~334 nm ($\epsilon = 1.0 \times 10^3$ M^{-1} cm^{-1}), 352 nm ($\epsilon = 7.96 \times 10^2$ M^{-1} cm^{-1}) and ~382 nm ($\epsilon = 1.69 \times 10^2$ M^{-1} cm^{-1}), assignable to the conjugated dibenzothiophene moiety. The spectrum also displayed a long absorption tail beginning around 350 and extending beyond 400 nm. This extended absorption tail beyond 400 nm indicates the compound's potential for excitation at longer wavelength, making it advantageous for cell-imaging applications. This property was later validated through confocal microscopy studies using HeLa cells. Therefore, DBT-FAA represents a promising candidate for site-specific incorporation into proteins for live-cell imaging.

3.3 Fluorescence spectroscopy and quantum yield

The fluorescence properties of 4-dibenzothiophen-4-yl-L-phenylalanine (DBT-FAA) were subsequently investigated. Upon excitation at 380 nm, 4-dibenzothiophen-4-yl-L-phenylalanine (in DMSO) exhibited a prominent emission peak at approximately 425 nm, accompanied by weaker shoulder peaks at ~452 nm, ~485 nm, and ~540 nm, with an emission tail extending up to 670 nm (Fig. 2). These emission features fall within the visible region, indicating the potential of DBT-AA for cellular imaging. When the DBT-FAA solution was illuminated at 365 nm under a UV lamp, the solution in quartz cuvette displayed a bright cyan fluorescence (Fig. 2, inset), confirming DBT-FAA is a cyan-emitting fluorescent amino acid.

The quantum yield of 4-dibenzothiophen-4-yl-L-phenylalanine (DBT-FAA) was determined using Williams' comparative method (SI). Rhodamine B in ethanol, with a known quantum yield ($\Phi_{ST} = 0.68$), was used as the reference standard (SI). Fluorescence emission spectra of Rhodamine B were recorded using an excitation wavelength of 420 nm and emission range of 450–800 nm, while DBT-FAA solutions (in DMSO) were excited at 380 nm and emission spectra were collected from 400 to 800 nm. For both samples, baseline-corrected integrated fluorescence intensity was plotted against absorbance for various concentrations, and the gradients (slopes) of the linear fits were obtained. The quantum yield of DBT-FAA (Φ_{ST}) was calculated using the equations provided in the SI and was determined to be 0.74.

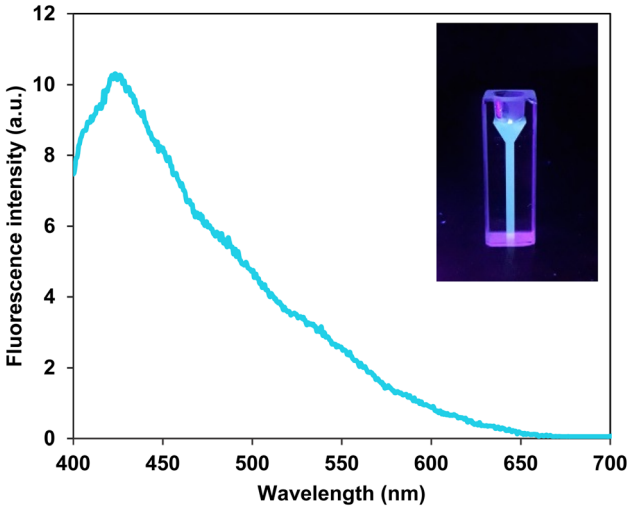

Fig. 2 Fluorescence spectrum of 4-dibenzothiophen-4-yl-L-phenylalanine (80 μM) in DMSO (excitation wavelength – 380 nm and emission collected from 400 nm to 700 nm). Inset is an image of 4-dibenzothiophen-4-yl-L-phenylalanine in DMSO solution in a quartz cuvette under UV illumination at 365 nm, showing the cyan light emission.

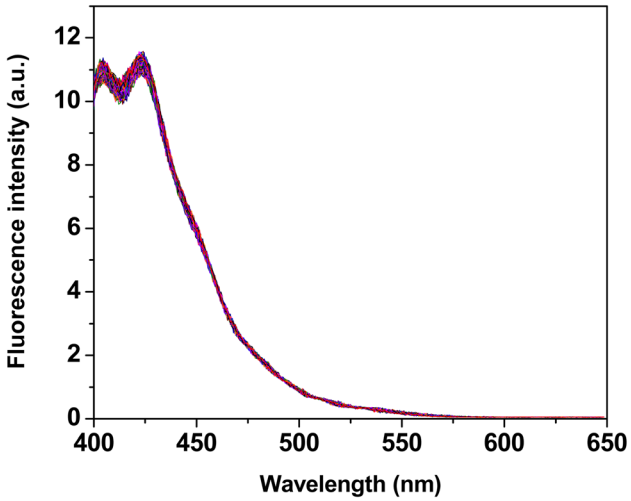

Fig. 3 Repeated scans of 100 fluorescence emission spectra (excitation wavelength (λ_{ex}) = 380 nm, emission wavelength = 400–650 nm, excitation slit 15 nm, emission slit 2.5 nm and scan speed = 250 nm min^{-1}) of 4-dibenzothiophen-4-yl-L-phenylalanine (DBT-FAA) (100 μM) over a 5 h period in DMSO–SPB buffer (1 : 1, pH 7.0, 0.05 M).

3.4 Photostability analysis

The photostability of 4-dibenzothiophen-4-yl-L-phenylalanine (DBT-FAA) was evaluated in a physiologically relevant buffer by recording a series of 100 fluorescence spectra over a period of 5 hours. The measurements were carried out using a 100 μM solution of the compound in a 1 : 1 mixture of DMSO and saline phosphate buffer (SPB, pH 7.0, 0.05 M), with excitation at wavelength 380 nm and emission monitored in the 400–650 nm range. DBT-FAA exhibited two major emission peaks at 403 and 424 nm, along with shoulder bands at approximately 448, 475, 513, and 582 nm. Interestingly, only a minimal decrease in fluorescence intensity was observed over the 5-hour duration – approximately 4.74% at 403 nm and ~3.64% at 424 nm – indicating strong resistance to photobleaching and excellent photostability under these conditions. This level of photostability is comparable to that of rhodamine B, which showed a 6.08% decrease in fluorescence intensity at its emission maximum (580 nm) after 100 scans over the same 5-hour duration under similar conditions (Fig. S4, SI).

3.5 Solvatochromic effects

4-Dibenzothiophen-4-yl-L-phenylalanine (DBT-FAA) exhibited slightly different fluorescence emission features in DMSO and DMSO–SPB buffer (see Fig. 2 and 3), indicating that solvent polarity influences its emission behavior. To further investigate this solvatochromic effect, fluorescence measurements were performed in a range of solvents with varying polarities, including acetone, methanol, ethanol, isopropanol, DMF, DMSO, water, Tris–HCl pH 8.8, 0.01 mM NaOH pH 9.0, and 0.02 mM NaOH pH 9.3.

As shown in Fig. 4 and Table S1 (in SI), DBT-FAA displayed the strongest emission in Tris–HCl buffer (pH 8.8), with a major emission peak at ~445 nm and shoulder bands at ~520 nm and ~582 nm. In DMSO, the compound showed a major emission peak at ~425 nm with shoulders at ~452 nm, ~485 nm, and ~540 nm. In isopropanol, a main peak at ~433 nm was observed along with shoulders at ~484 nm and ~555 nm, while in methanol, the major peak appeared at ~433 nm with shoulders at ~466 nm and ~550 nm. DBT-FAA in acetone showed a similar pattern, with a principal peak at ~433 nm and shoulders at ~484 nm and ~532 nm. In DMF, a main emission at ~434 nm was accompanied by shoulders at ~484 nm and ~548 nm. In 0.01 mM NaOH (pH 9.0) and 0.02 mM NaOH (pH 9.3), the emission maximum appeared at ~431 nm with

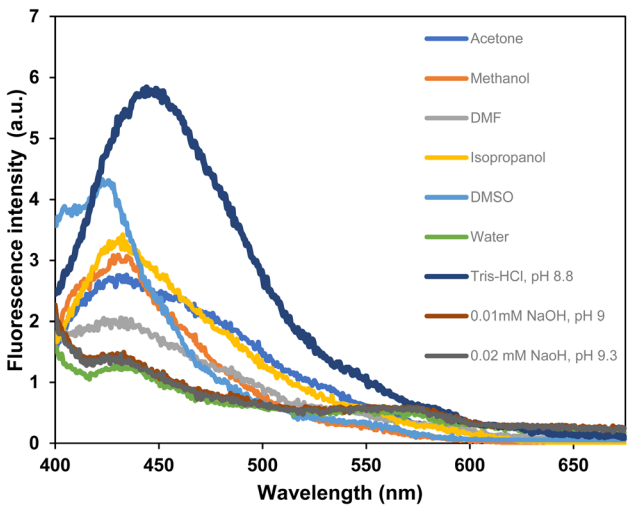

Fig. 4 Fluorescence emission spectra of 4-dibenzothiophen-4-yl-L-phenylalanine (DBT-FAA) (20 μM) (excitation wavelength, λ_{ex} = 380 nm, emission wavelength = 400–675 nm, excitation slit 15 nm, emission slit 2.5 nm and scan speed = 250 nm min^{-1}) in different solvents.

shoulders at ~454 nm and ~484 nm, and weaker bands at ~550 nm and ~582 nm. In water, a major emission peak at ~433 nm was observed with shoulders at ~460 nm and ~496 nm, and a weak band around ~580 nm.

Solvatochromism is a complex phenomenon governed by the interplay of multiple factors, including solvent dielectric constant, hydrogen-bonding interactions, solvent polarization effects, solvent-induced conformational changes, and solute aggregation.[47] These interactions can alter the relative energies of the electronic ground and excited states, leading to shifts in the emission spectrum. Given that DBT-FAA contains multiple functional groups, it is likely that several of these factors contribute to its observed solvatochromic behavior.

Notably, the fluorescence emission of DBT-FAA was most pronounced (higher intensity and longer emission wavelength) in Tris–HCl buffer (pH 8.8), a physiologically relevant medium, suggesting that DBT-FAA possesses desirable fluorescence characteristics for biological and cellular imaging applications.

3.6 Optical rotation measurement

The optical rotation (α) of 4-dibenzothiophen-4-yl-L-phenylalanine (DBT-FAA) (10 mM in DMSO), was measured, and the specific rotation ($[\alpha]$) was calculated using the following equation:

$$[\alpha]_{\lambda}^{T} = \frac{\alpha \times 100}{c \times l}$$

where, α = observed optical rotation (°), c = concentration in g/100 ml, and l = path length in decimeters.

Substituting the experimental values:

$$[\alpha]_{\lambda}^{T} = \frac{-0.084 \times 100}{0.3414025 \times 1} = -24.60^{\circ}$$

Thus, the specific rotation of 4-dibenzothiophen-4-yl-L-phenylalanine was determined to be $[\alpha]_{589}^{25.1} = -24.6°$ (measured at 25.1 °C and 589 nm). This value closely matches those reported for the blue-emitting fluorescent amino acid 4-phenanthracen-9-yl-L-phenylalanine[39] and for L-phenylalanine, confirming that DBT-FAA possesses the L-configuration.

3.7 Cytotoxicity and cellular imaging studies

To further evaluate the fluorescence capability and potential cytotoxicity of 4-dibenzothiophen-4-yl-L-phenylalanine (DBT-FAA), experiments were conducted in living human HeLa

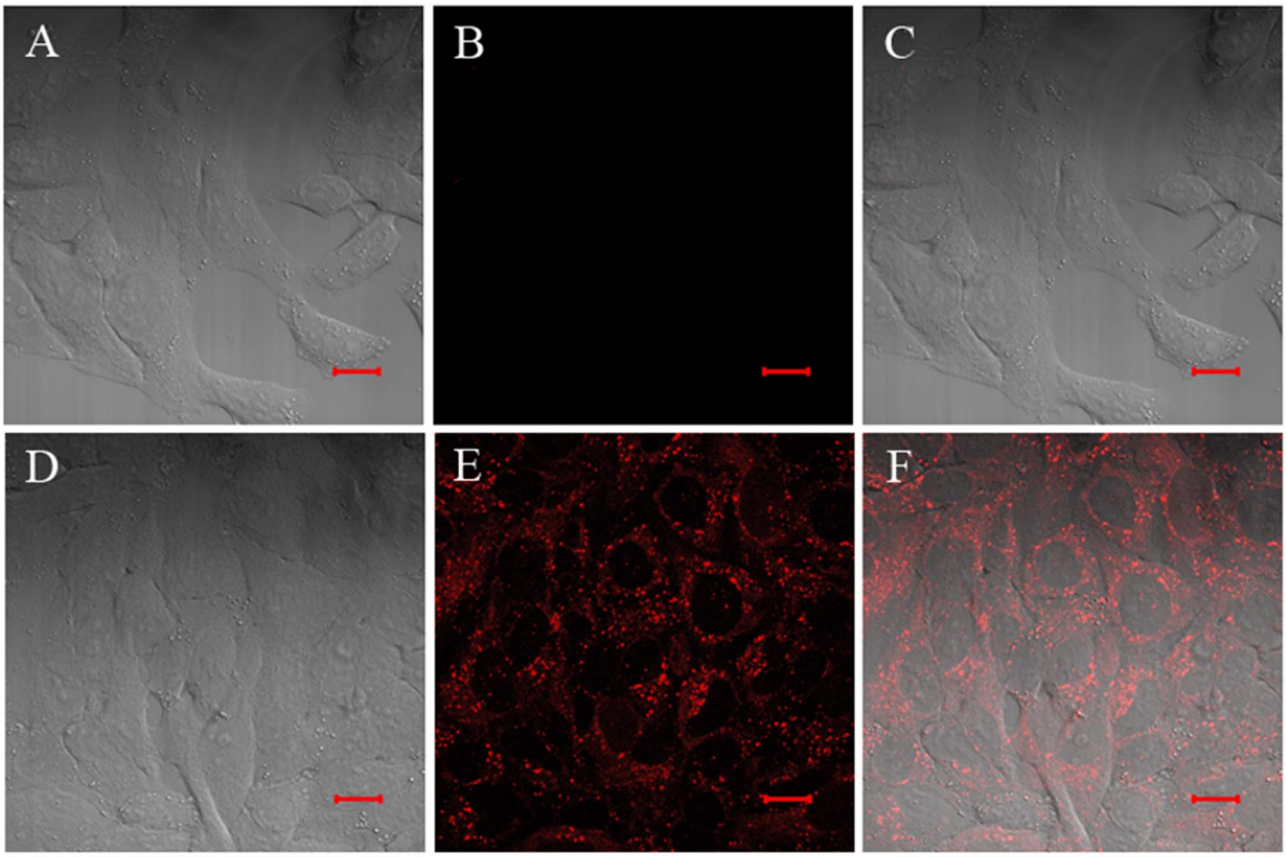

Fig. 5 Confocal images of HeLa cells treated or untreated with DBT-FAA. (A–C) Control HeLa cells without FAA treatment. (D–F) HeLa cells treated with DBT-FAA at a final concentration of 20 μM. (A and D) were bright field images; (B and E) were fluorescent images after excitation at 405 nm and emission collected between 410 and 587 nm; (C and F) were merged with bright-field and fluorescence signals. The fluorescence signals (red pseudo-color) in (E) indicate that DBT-FAA readily permeates live cells and exhibits strong intracellular fluorescence. Scale bar: 20 μm.

cells. Cells were treated with DBT-FAA at final concentrations of 10 μM, 20 μM, and 50 μM, respectively. After a 1-hour incubation period, the culture medium was replaced with fresh medium to remove any residual background fluorescence prior to confocal imaging.

Confocal imaging of DBT-FAA was performed using a Zeiss LSM 710 laser confocal microscope with excitation at 405 nm, a wavelength that corresponds to the absorption tail of DBT-FAA, as reported previously.[39] Cells incubated with 10 μM or 20 μM DBT-FAA exhibited strong cytosolic fluorescence signals (shown in red pseudo-color; Fig. 5 and S6), with no noticeable changes in cell morphology or viability compared with untreated controls. As the DBT-FAA concentration increased, cells continued to display normal morphology, indicating minimal cytotoxicity even at 50 μM (Fig. S7).

The *in vitro* cytotoxicity of DBT-FAA was further evaluated using a standard MTT assay with WS1 cells (human skin primary fibroblasts). As shown in Fig. S5 (SI), WS1 cells were incubated with DBT-FAA at concentrations ranging from 0 to 50 μM for 24 h. No detectable cytotoxicity was observed at any of the concentrations tested; instead, a slight enhancement in cell viability was noted. Collectively, these results demonstrate that DBT-FAA can efficiently label living cells while maintaining excellent biocompatibility.

To investigate the subcellular localization of DBT-FAA in HeLa cells, organelle-specific fluorescent probes were employed. As shown in Fig. 6, mitochondria and lysosomes were stained with green and blue fluorescent markers, respectively. The distinct separation of green and red (pseudo-colors) fluorescence in Fig. 6E indicates that although DBT-FAA was distributed in the cytosol, it did not predominantly accumulate within the mitochondria following a 30-minute incubation period. In contrast, the merged image in Fig. 6F displayed extensive overlap between the red and blue (pseudo-colors) fluorescence signals, producing a pronounced purple hue. This co-localization pattern strongly suggests that DBT-FAA is preferentially localized within lysosomes. The observed intracellular distribution implies that DBT-FAA is likely internalized through an endocytic pathway, similar to that of leucine or phenylalanine,[52] subsequently accumulating in lysosomal compartments.

To investigate the kinetics of DBT-FAA interaction with HeLa cells, cells were incubated with 4-dibenzothiophen-4-yl-L-phenylalanine (DBT-FAA) at a final concentration of 20 μM for 90 min, 3 h, 6 h, 12 h, and 24 h, respectively. Mitochondrial and lysosomal trackers were added 30 min prior to imaging. As shown in Fig. S8E–H, in additional to purple fluorescence signals indicating co-localization of DBT-FAA with the lysosomal tracker, distinguishable orangish-yellow signals were observed at later time points (panels F and G), consistent with co-localization of DBT-FAA with the mitochondrial tracker and suggesting mitochondria localization.

With extended incubation times (3–24 h), the degree of co-localization between DBT-FAA (red pseudo-color) and the mitochondrial tracker (green pseudo-color) gradually increased, producing orangish-yellow signals in the merged images

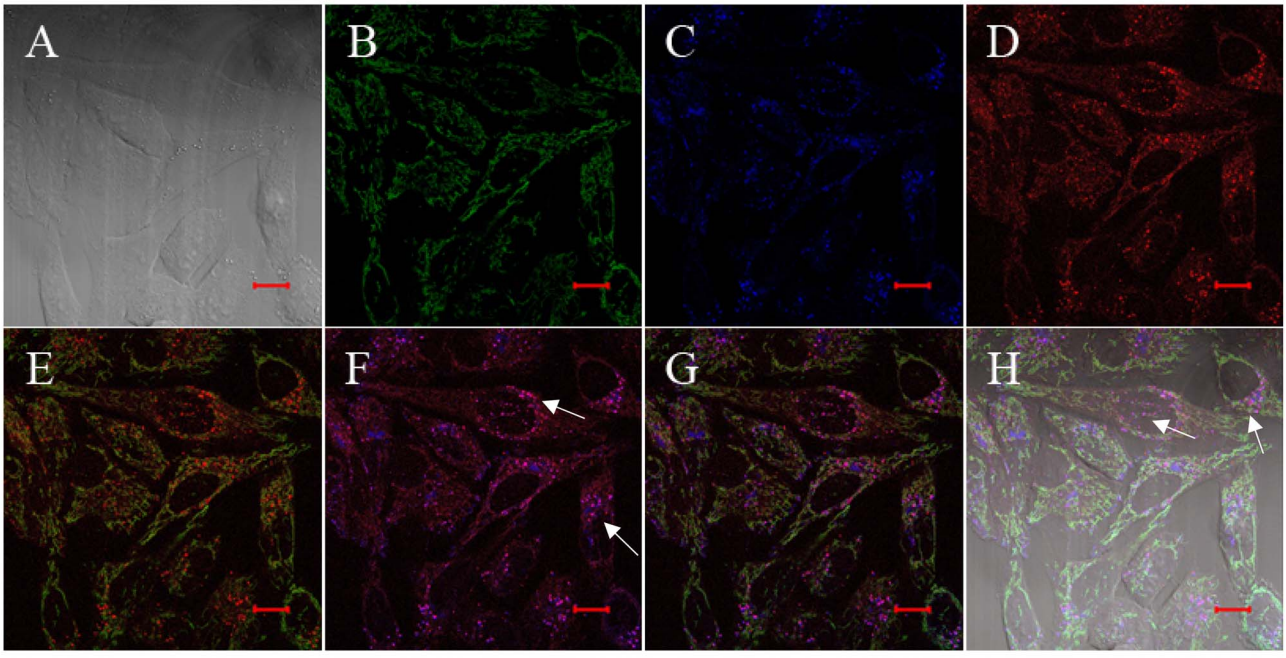

Fig. 6 Confocal images of HeLa cells treated with DBT-FAA (red pseudo-color) for 30 min, followed by incubation with mitochondria tracker (green pseudo-color) and lysosome tracker (blue pseudo-color). (A) Bright-field image of cells; (B) fluorescence images of mitochondria after (excitation at 488 nm, emission 493–620 nm); (C) fluorescence image of lysosomes (excitation at 543 nm, emission 566–690 nm); (D) fluorescent image of DBT-FAA (excitation at 405 nm, emission 410–587 nm). (E and F) Co-localization of DBT-FAA with mitochondrial and lysosomal signals, respectively; (G) merged fluorescence image showing DBT-FAA, mitochondria, and lysosomes; (H) merged image of DBT-FAA, mitochondria, and lysosomes overlaid with bright-field view. Scale bar: 20 μm.

(Fig. 7F and G, 8F and G; S9F, G, S10F and G). These observations indicate a time-dependent redistribution of DBT-FAA from the cytosol and lysosomes toward the mitochondria.

Fig. S11 presents a quantitative analysis of colocalization in the confocal images, showing the relative distributions of DBT-FAA in lysosomes and mitochondria over time (30 min to 24 h). At 30 min, DBT-FAA was dominantly localized in lysosomes with minimal mitochondria association. By 90 min, lysosomal DBT-FAA decreased markedly, accompanied by a corresponding increase in mitochondrial DBT-FAA. Mitochondrial colocalization continued to increase, surpassing lysosomal levels at 6 h and reaching a plateau after 12 h. In contrast, lysosomal DBT-FAA increased slowly from 90 min to 12 h and decreased slightly after 24 h, likely reflecting continued cellular uptake of DBT-FAA from the culture medium.

Collectively, these results suggest that DBT-FAA is bioavailable within mitochondria and may participate in mitochondrial protein-associated processes, although direct evidence for incorporation into mitochondrial proteins will require further investigation.

A closer inspection of the images in Fig. 7, 8, and S8–S10 suggests the presence of close contacts between the two organelles during the DBT-FAA translocation process. Increasing evidence supports the existence of dynamic lysosome–mitochondria contact sites that facilitate localized signaling and metabolite exchange, including calcium and small-molecule transfer.[48] Notably, direct contacts between mitochondria and lysosomes – distinct from those associated with mitophagy[49,50] or mitochondrial-derived vesicles (MDVs) – have been observed in healthy cells.[51] Such close contacts may enable efficient exchange of metabolites or essential nutrient molecules between the two organelles.[48,51]

Cells acquire nutrients from their environment and utilize them in various metabolic pathways, especially when resources are scarce. Several large neutral or aromatic amino acids, such as leucine and phenylalanine, have been shown to enter cells *via* endocytosis mediated by the L-type amino acid transporter 1 (LAT1) and become transiently stored in lysosomes, from which they can subsequently be mobilized for protein synthesis.[52,53] Seven amino acids—leucine, valine, isoleucine, tyrosine, phenylalanine, methionine, and tryptophan are exported from lysosomes in an mTORC1-dependent manner.[54] DBT-FAA (4-dibenzothiophen-4-yl-L-phenylalanine), a phenylalanine derivative bearing an extended aromatic side chain, shares structural features with these amino acids and therefore may follow a similar cellular uptake and trafficking route. Consistent with this possibility, our imaging data show intracellular accumulation of DBT-FAA in lysosomal compartments. While no direct evidence is provided here for the specific involvement of LAT1 or endocytosis, the observed lysosomal localization aligns with previously reported behavior of large neutral amino acids.

Moreover, the time-dependent redistribution of DBT-FAA from lysosomes to mitochondria suggests that the compound is not permanently sequestered and remains bioavailable to other

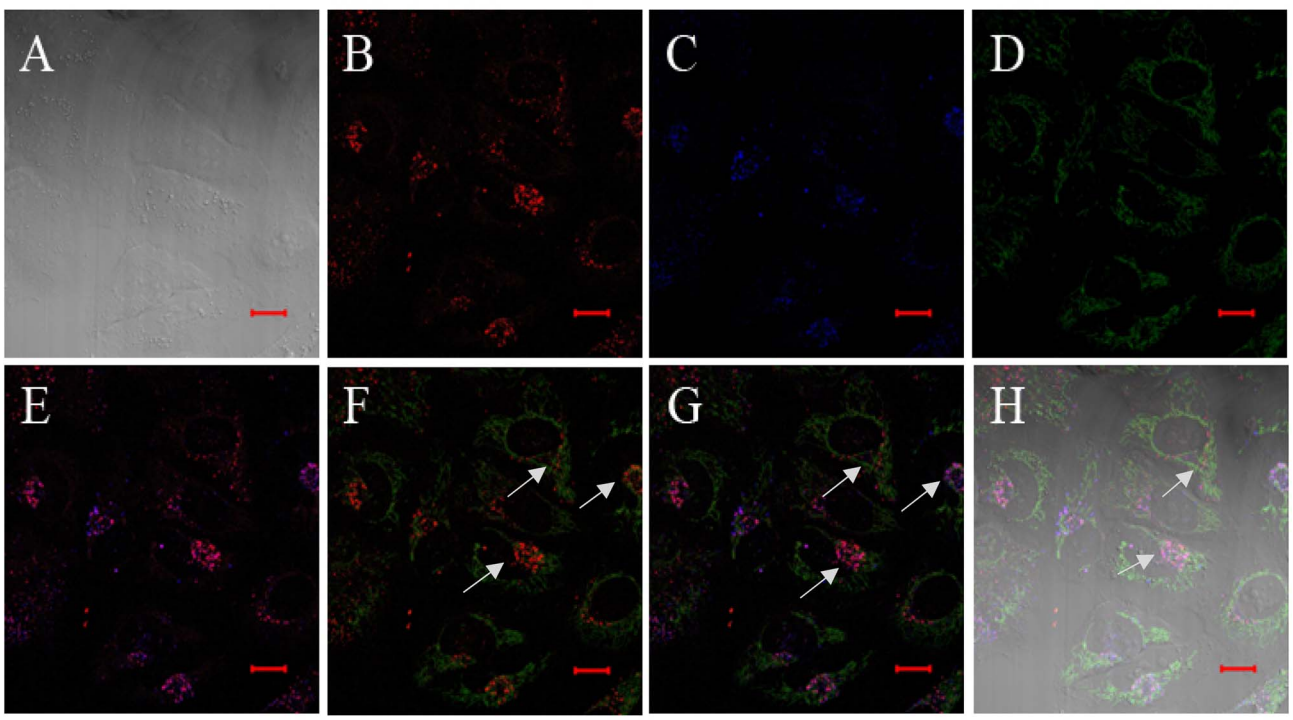

Fig. 7 Confocal images of HeLa cells treated with DBT-FAA (red pseudo-color) for 3 h, followed by incubation with mitoTracker (green pseudo-color) and lysoTracker (blue pseudo-color) for 30 min prior to imaging. (A) Bright-field image of cells; (B) fluorescent images of DBT-FAA (excitation at 405 nm, emission 410–587 nm); (C) fluorescent image of lysosomes (excitation at 543 nm, emission 566–690 nm); (D) fluorescence image of mitochondria (excitation at 488 nm. Emission 493–620 nm). (E and F) Co-localization of DBT-FAA with lysosomal and mitochondrial fluorescent signals, respectively; (G) merged fluorescent image showing DBT-FAA, mitochondria, and lysosomes; (H) merged fluorescent image of DBT-FAA, mitochondria, and lysosomes overlaid with the bright-field view. Scale bar: 20 μm.

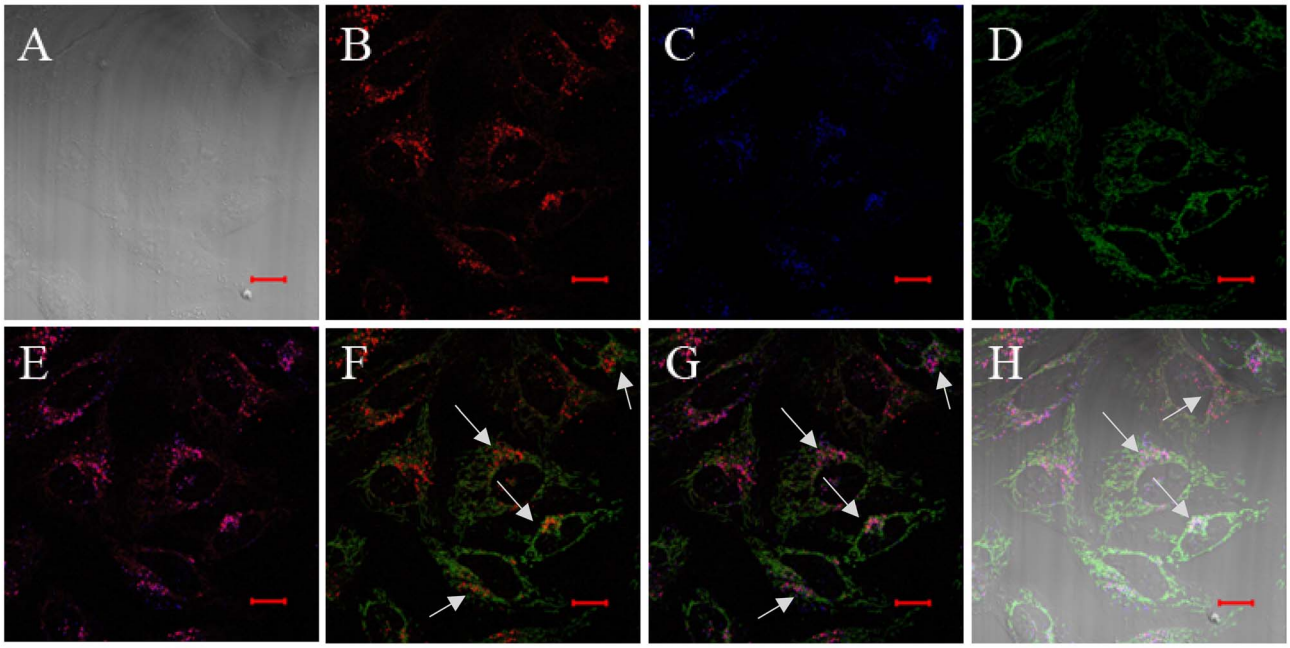

Fig. 8 Confocal images of HeLa cells treated with DBT-FAA (red pseudo-color) for 24 h, followed by incubation with mitoTracker (green pseudo-color) and lysoTracker (blue pseudo-color) for 30 min prior to imaging. (A) Bright-field image of cells; (B) fluorescent images of DBT-FAA (excitation at 405 nm, emission 410–587 nm); (C) fluorescent image of lysosomes (excitation at 543 nm, emission 566–690 nm); (D) fluorescence image of mitochondria (excitation at 488 nm, emission 493–620 nm). (E and F) Co-localization of DBT-FAA with mitochondrial and lysosomal fluorescent signals, respectively; (G) merged fluorescent image showing DBT-FAA, mitochondria, and lysosomes; (H) merged fluorescent image of DBT-FAA, mitochondria, and lysosomes overlaid with the bright-field view. Scale bar: 20 μm.

organelles. Together, these observations support the hypothesis that DBT-FAA may participate in amino acid – like intracellular trafficking pathways and could potentially be accessible for utilization in other cellular compartments, although direct mechanistic validation will be required in future studies.

3.8 Comparison with previously reported visible-emitting FAAs

The photophysical properties and biological applications of the fluorescent amino acid DBT-FAA were compared with those of previously reported representative visible-emitting fluorescent amino acids, as summarized in Table S2 (SI). Only a limited number of visible-emitting fluorescent amino acids have been reported, and many of them are unsuitable for bioimaging due to low quantum yields or other limitations. This comparison highlights several notable advantages of DBT-FAA, including a high quantum yield, high photostability, excitable by a 405 nm laser and emission wavelengths within the true visible region, as well as excellent biocompatibility, making it a promising candidate for incorporation into peptides or proteins for bioimaging applications.

4. Conclusions

In summary, a novel cyan-emitting fluorescent α-amino acid, 4-dibenzothiophen-4-yl-L-phenylalanine (DBT-FAA) was designed and successfully synthesized in good yield *via* a modified Suzuki–Miyaura cross-coupling reaction. DBT-FAA exhibited strong fluorescence in a broad range of aqueous and polar solvents, with a major emission peak at ~425 nm and secondary shoulders at longer wavelengths, along with a high quantum yield ($\Phi = 0.74$). It also demonstrated excellent photostability, showing strong resistance to photobleaching under aqueous conditions. DBT-FAA was readily taken up by human HeLa cells and produced bright fluorescence under 405 nm laser excitation, as observed by confocal microscopy. Co-localization experiments revealed that DBT-FAA enters cells readily with an initial accumulation in lysosomes and subsequently translocated to mitochondria with prolonged incubation. The successful cellular uptake and cyan-emitting fluorescence of this novel amino acid highlight its promise as a bioimaging probe, offering new opportunities for studying protein folding, dynamics, and intermolecular interactions—ultimately advancing protein engineering, drug discovery, and therapeutic design.

Author contributions

Aakash Gupta: writing – review & editing, writing – original draft, methodology, investigation, formal analysis, data curation. Bing Yan: visualization, methodology, investigation, formal analysis, data curation. Yu Hsiang Cheng: methodology, investigation, formal analysis, data curation. Maolin Guo: writing – review & editing, writing – original draft, supervision,

project administration, methodology, investigation, funding acquisition, formal analysis, data curation, conceptualization.

Conflicts of interest

The authors declare that they have no competing financial interests nor personal relationships with the work described in this manuscript.

Data availability

Supplementary information (SI): experimental procedures, characterization data (NMR, mass spectrometry, fluorescence properties), and additional cell imaging results. See DOI: https://doi.org/10.1039/d5ra09861k.

Acknowledgements

We acknowledge Dr Y. Wei for technical assistance and the NSF (CHE-1229339), NIH (1R15GM126576-01), the Orphan Disease Center/Loulou foundation, and University of Massachusetts Dartmouth Seed Funding Program for funding.

References

1 O. Shimomura, F. H. Johnson and Y. Saiga, Extraction, purification and properties of aequorin, a bioluminescent protein from the luminous hydromedusan, Aequorea, *J. Cell. Comp. Physiol.*, 1962, **59**, 223–239, DOI: 10.1002/jcp.1030590302.

2 R. Y. Tsien, The green fluorescent protein, *Annu. Rev. Biochem.*, 2003, **67**, 509–544, DOI: 10.1146/ANNUREV.BIOCHEM.67.1.509.

3 M. Chalfie, Y. Tu, G. Euskirchen, W. W. Ward and D. C. Prasher, Green fluorescent protein as a marker for gene expression, *Science*, 1994, **263**, 802–805, DOI: 10.1126/science.8303295.

4 C. J. Weijer, Visualizing signals moving in cells, *Science*, 2003, **300**, 96–100, DOI: 10.1126/science.1082830.

5 B. N. G. Giepmans, S. R. Adams, M. H. Ellisman and R. Y. Tsien, The fluorescent toolbox for assessing protein location and function, *Science*, 2006, **312**, 217–224, DOI: 10.1126/science.1124618.

6 M. J. Pittet and R. Weissleder, Intravital imaging, *Cell*, 2011, **147**, 983–991, DOI: 10.1016/j.cell.2011.11.004.

7 R. N. Germain, E. A. Robey and M. D. Cahalan, A decade of imaging cellular motility and interaction dynamics in the immune system, *Science*, 2012, **336**, 1676–1681, DOI: 10.1126/science.1221063.

8 A. Keppler, S. Gendreizig, T. Gronemeyer, H. Pick, H. Vogel and K. Johnsson, A general method for the covalent labeling of fusion proteins with small molecules in vivo, *Nat. Biotechnol.*, 2003, **21**, 86–89, DOI: 10.1038/nbt765.

9 X. Sun, A. Zhang, B. Baker, L. Sun, A. Howard, J. Buswell, D. Maurel, A. Masharina, K. Johnsson, C. J. Noren, M.-Q. Xu and I. R. Corrêa, Development of SNAP-Tag Fluorogenic Probes for Wash-Free Fluorescence Imaging, *ChemBioChem*, 2011, **12**, 2217–2226, DOI: 10.1002/cbic.201100173.

10 T. Komatsu, K. Johnsson, H. Okuno, H. Bito, T. Inoue, T. Nagano and Y. Urano, Real-time measurements of protein dynamics using fluorescence activation-coupled protein labeling method, *J. Am. Chem. Soc.*, 2011, **133**, 6745–6751, DOI: 10.1021/JA200225M.

11 A. Gautier, A. Juillerat, C. Heinis, I. R. Corrêa, M. Kindermann, F. Beaufils and K. Johnsson, An Engineered Protein Tag for Multiprotein Labeling in Living Cells, *Chem. Biol.*, 2008, **15**, 128–136, DOI: 10.1016/J.CHEMBIOL.2008.01.007.

12 G. v Los, L. P. Encell, M. G. Mcdougall, D. D. Hartzell, N. Karassina, C. Zimprich, M. G. Wood, R. Learish, R. Friedman Ohana, M. Urh, D. Simpson, J. Mendez, K. Zimmerman, P. Otto, G. Vidugiris, J. Zhu, A. Darzins, D. H. Klaubert, R. F. Bulleit and K. v Wood, HaloTag: A Novel Protein Labeling Technology for Cell Imaging and Protein Analysis, *ACS Chem. Biol.*, 2008, **3**, 373–382, DOI: 10.1021/cb800025k.

13 E. I. Kovalenko, S. Ranjbar, L. D. Jasenosky, A. E. Goldfeld, I. A. Vorobjev and N. S. Barteneva, The use of HaloTag-based technology in flow and laser scanning cytometry analysis of live and fixed cells, *BMC Res. Notes*, 2011, **4**, 340, DOI: 10.1186/1756-0500-4-340.

14 L. W. Miller, Y. Cai, M. P. Sheetz and V. W. Cornish, In vivo protein labeling with trimethoprim conjugates: a flexible chemical tag, *Nat. Methods*, 2005, **2**, 255–257, DOI: 10.1038/nmeth749.

15 D. P. Baccanari, S. Daluge and R. W. King, Inhibition of Dihydrofolate Reductase: Effect of Reduced Nicotinamide Adenine Dinucleotide Phosphate on the Selectivity and Affinity of Diaminobenzylpyrimidines, *Biochemistry*, 1982, **21**, 5068–5075, DOI: 10.1021/bi00263a034.

16 R. Wombacher, M. Heidbreder, S. van de Linde, M. P. Sheetz, M. Heilemann, V. W. Cornish and M. Sauer, Live-cell super-resolution imaging with trimethoprim conjugates, *Nat. Methods*, 2010, **7**, 717–719, DOI: 10.1038/nmeth.1489.

17 S. S. Gallaghers, C. Jing, D. S. Peterka, M. Konate, R. Wombacher, L. J. Kaufman, R. Yuste and V. W. Cornish, A trimethoprim-based chemical tag for live cell two-photon imaging, *Chembiochem*, 2010, **11**, 782–784, DOI: 10.1002/CBIC.200900731.

18 B. A. Griffin, S. R. Adams and R. Y. Tsien, Specific covalent labeling of recombinant protein molecules inside live cells, *Science*, 1998, **281**, 269–272, DOI: 10.1126/SCIENCE.281.5374.269/ASSET/B7F6729A-062D-4A34-88A6-B4F46A378155/ASSETS/GRAPHIC/SE2886670004.JPEG.

19 A. T. Krueger and B. Imperiali, Fluorescent Amino Acids: Modular Building Blocks for the Assembly of New Tools for Chemical Biology, *ChemBioChem*, 2013, **14**, 788–799, DOI: 10.1002/CBIC.201300079.

20 A. Adhikari, B. R. Bhattarai, A. Aryal, N. Thapa, K. C. Puja, A. Adhikari, S. Maharjan, P. B. Chanda, B. P. Regmi and N. Parajuli, Reprogramming natural proteins using unnatural amino acids, *RSC Adv.*, 2021, **11**, 38126–38245, DOI: 10.1039/d1ra07028b.

21 O. Marshall and A. Sutherland, Expanding the fluorescence toolkit: molecular design, synthesis and biological application of unnatural amino acids, *Chem. Sci.*, 2025, **16**, 16414–16432, DOI: 10.1039/d5sc05745k.

22 Z. Cheng, E. Kuru, A. Sachdeva and M. Vendrell, Fluorescent amino acids as versatile building blocks for chemical biology, *Nat. Rev. Chem.*, 2020, **4**, 275–290, DOI: 10.1038/s41570-020-0186-z.

23 J. Wang, J. Xie and P. G. Schultz, A genetically encoded fluorescent amino acid, *J. Am. Chem. Soc.*, 2006, **128**, 8738–8739, DOI: 10.1021/JA062666K/SUPPL_FILE/JA062666KSI20060531_034715.PDF.

24 A. Chatterjee, J. Guo, H. S. Lee and P. G. Schultz, A genetically encoded fluorescent probe in mammalian cells, *J. Am. Chem. Soc.*, 2013, **135**, 12540–12543, DOI: 10.1021/JA4059553/SUPPL_FILE/JA4059553_SI_001.PDF.

25 M. R. Hilaire, I. A. Ahmed, C. W. Lin, H. Jo, W. F. DeGrado and F. Gai, Blue fluorescent amino acid for biological spectroscopy and microscopy, *Proc. Natl. Acad. Sci. U.S.A.*, 2017, **114**, 6005–6009, DOI: 10.1073/PNAS.1705586114/SUPPL_FILE/PNAS.201705586SI.PDF.

26 R. Clarke, L. Zeng, B. C. Atkinson, M. Kadodwala, A. R. Thomson and A. Sutherland, Fluorescent carbazole-derived a-amino acids: structural mimics of tryptophan, *Chem. Sci.*, 2024, **15**, 5944, DOI: 10.1039/d4sc01173brsc.li/chemical-science.

27 J. S. Lampkowski, D. M. Uthappa and D. D. Young, Site-specific incorporation of a fluorescent terphenyl unnatural amino acid, *Bioorg. Med. Chem. Lett.*, 2015, **25**, 5277–5280, DOI: 10.1016/J.BMCL.2015.09.050.

28 E. J. Watkins, P. J. Almhjell and F. H. Arnold, Direct enzymatic synthesis of a deep-blue fluorescent noncanonical amino acid from azulene and serine, *ChemBioChem*, 2020, **21**, 80–83, DOI: 10.1002/CBIC.201900497.

29 J. Lee, K. J. Schwarz, H. Yu, A. Krüger, E. v. Anslyn, A. D. Ellington, J. S. Moore and M. C. Jewett, Ribosome-mediated incorporation of fluorescent amino acids into peptidesin vitro, *Chem. Commun.*, 2021, **57**, 2661–2664, DOI: 10.1039/d0cc07740b.

30 S. L. Hyun, J. Guo, E. A. Lemke, R. D. Dimla and P. G. Schultz, Genetic incorporation of a small, environmentally sensitive, fluorescent probe into proteins in Saccharomyces cerevisiae, *J. Am. Chem. Soc.*, 2009, **131**, 12921–12923, DOI: 10.1021/JA904896S/SUPPL_FILE/JA904896S_SI_001.PDF.

31 R. Feng, M. Wang, W. Zhang and F. Gai, Unnatural Amino Acids for Biological Spectroscopy and Microscopy, *Chem. Rev.*, 2024, **124**, 6501–6542, DOI: 10.1021/acs.chemrev.3c00944.

32 Y. Wei, Y. Zhang, Z. Liu and M. Guo, A novel profluorescent probe for detecting oxidative stress induced by metal and H2O2 in living cells, *Chem. Commun.*, 2010, **46**, 4472–4474, DOI: 10.1039/C000254B.

33 Y. Wei, Z. Aydin, Y. Zhang, Z. Liu and M. Guo, A Turn-on Fluorescent Sensor for Imaging Labile Fe^{3+} in Live Neuronal Cells at Subcellular Resolution, *ChemBioChem*, 2012, **13**, 1569–1573, DOI: 10.1002/CBIC.201200202.

34 S. Maiti, Z. Aydin, Y. Zhang and M. Guo, Reaction-based turn-on fluorescent probes with magnetic responses for Fe^{2+} detection in live cells, *Dalton Trans.*, 2015, **44**, 8942–8949, DOI: 10.1039/C4DT03792H.

35 Z. Aydin, Y. Wei and M. Guo, An "off–on" optical sensor for mercury ion detection in aqueous solution and living cells, *Inorg. Chem. Commun.*, 2014, **50**, 84–87, DOI: 10.1016/j.inoche.2014.10.026.

36 B. P. Garreffi, M. Guo, N. Tokranova, N. C. Cady, J. Castracane and I. A. Levitsky, Highly sensitive and selective fluorescence sensor based on nanoporous silicon-quinoline composite for trace detection of hydrogen peroxide vapors, *Sens. Actuators, B*, 2018, **276**, 466–471, DOI: 10.1016/J.SNB.2018.07.115.

37 Z. Aydin, B. Yan, Y. Wei and M. Guo, A novel near-infrared turn-on and ratiometric fluorescent probe capable of copper(II) ion determination in living cells, *Chem. Commun.*, 2020, **56**, 6043–6046, DOI: 10.1039/D0CC01481H.

38 Z. Liu, *Genetically Encoded Incorporation of Unnatural Fluorescent Amino Acids into Proteins for Molecular Imaging in Living Cells*, University of Massachusetts Dartmouth/Lowell, 2016.

39 A. Gupta, B. P. Garreffi and M. Guo, Facile Synthesis of a Novel Genetically Encodable Fluorescent α-Amino Acid Emitting Greenish Blue Light, *Chem. Commun.*, 2020, **56**, 12578–12581, DOI: 10.1039/D0CC03643A.

40 A. Gupta, B. Yan and M. Guo, Synthesis, Characterization, and Cellular Imaging of a Cyan Emitting Fluorescent Alpha-Amino Acid for Live-Cell Protein Imaging, in *Protein Science*, Wiley, 111 RIVER ST, HOBOKEN 07030-5774, NJ USA, 2023.

41 A. Gupta, B. Yan and M. Guo, Synthesis, characterization, and cellular imaging of a novel cyan emitting fluorescent α-amino acid, *J. Biol. Chem.*, 2023, **299**, 103251.

42 C. Zhang, J. Huang, M. L. Trudell and S. P. Nolan, Palladium-imidazol-2-ylidene complexes as catalysts for facile and efficient Suzuki cross-coupling reactions of aryl chlorides with arylboronic acids, *J. Org. Chem.*, 1999, **64**, 3804–3805, DOI: 10.1021/jo990554o.

43 S. Kotha and K. Lahiri, Application of the Suzuki-Miyaura cross-coupling reaction for the modification of phenylalanine peptides, *Biopolymers*, 2003, **69**, 517–528, DOI: 10.1002/bip.10420.

44 S. Chen, N. E. Fahmi, C. Bhattacharya, L. Wang, Y. Jin, S. J. Benkovic and S. M. Hecht, Fluorescent Biphenyl Derivatives of Phenylalanine Suitable for Protein Modification, *Biochemistry*, 2013, **52**, 8580–8589, DOI: 10.1021/bi401275v.

45 N. Budisa, S. Alefelder, J. H. Bae, R. Golbik, C. Minks, R. Huber and L. Moroder, Proteins with β-(thienopyrrolyl) alanines as alternative chromophores and pharmaceutically active amino acids, *Protein Sci.*, 2001, **10**, 1281–1292, DOI: 10.1110/PS.51601.

46 C. W. Bird, A new aromaticity index and its application to five-membered ring heterocycles, *Tetrahedron*, 1985, **41**, 1409–1414, DOI: 10.1016/S0040-4020(01)96543-3.

47 A. Marini, A. Muñoz-Losa, A. Biancardi and B. Mennucci, What is solvatochromism?, *J. Phys. Chem. B*, 2010, **114**, 17128–17135, DOI: 10.1021/JP1097487/SUPPL_FILE/JP1097487_SI_001.PDF.

48 A. Jain and R. Zoncu, Organelle transporters and inter-organelle communication as drivers of metabolic regulation and cellular homeostasis, *Mol. Metab.*, 2022, **60**, 101481, DOI: 10.1016/j.molmet.2022.101481.

49 S. Auguste, B. Yan and M. Guo, Induction of mitophagy by green tea extracts and tea polyphenols: A potential anti-aging mechanism of tea, *Food Biosci.*, 2023, **55**, 102983, DOI: 10.1016/j.fbio.2023.102983.

50 S. Auguste, B. Yan, R. Magina, L. Xue, C. Neto and M. Guo, Cranberry extracts and cranberry polyphenols induce mitophagy in human fibroblast cells, *Food Biosci.*, 2024, **57**, 103549, DOI: 10.1016/j.fbio.2023.103549.

51 W. Peng, Y. C. Wong and D. Krainc, Mitochondria-lysosome contacts regulate mitochondrial Ca^{2+} dynamics *via* lysosomal TRPML1, *Proc. Natl. Acad. Sci. U. S. A.*, 2020, **117**, 19266–19275, DOI: 10.1073/pnas.2003236117.

52 K. Tae, S.-J. Kim, S.-W. Cho, H. Lee, H.-S. Cha and C.-Y. Choi, L-Type Amino Acid Transporter 1 (LAT1) Promotes PMA-Induced Cell Migration through mTORC2 Activation at the Lysosome, *Cells*, 2023, **12**, 2504, DOI: 10.3390/cells12202504.

53 U. Bandyopadhyay, P. Todorova, N. N. Pavlova, Y. Tada, C. B. Thompson, L. W. S. Finley and M. Overholtzer, Leucine retention in lysosomes is regulated by starvation, *Proc. Natl. Acad. Sci. U. S. A.*, 2022, **119**, e2114912119, DOI: 10.1073/pnas.2114912119.

54 G. A. Wyant, M. Abu-Remaileh, R. L. Wolfson, W. W. Chen, E. Freinkman, L. V. Danai, M. G. Vander Heiden and D. M. Sabatini, mTORC1 Activator SLC38A9 Is Required to Efflux Essential Amino Acids from Lysosomes and Use Protein as a Nutrient, *Cell*, 2017, **171**, 642–654, DOI: 10.1016/j.cell.2017.09.046.